Powder Processing and Properties of Zircon-Reinforced Al-13.5Si-2.5Mg Alloy Composites

J.U. Ejiofor, B.A. Okorie, and R.G. Reddy

Zircon, $ZrSiO_4$, is a thermally stable mineral requiring expensive and energy-intensive process to reduce. Owing to its abundance, high hardness, excellent abrasion/wear resistance, and low coefficient of thermal expansion, a low-cost alternative use of the mineral for medium-strength tribology was investigated. The present study has developed a conventional low-cost, double-compaction powder metallurgy route in the synthesis of Al-13.5Si-2.5Mg alloy reinforced with zircon. The mechanical and physical properties were determined following the development of optimum conditions of cold pressing and reaction sintering. Reinforcing the hypereutectic Al-Si alloy with 15 vol% zircon particles (size < 200 μm) and cold pressing at 350 MPa to near-net shape, followed by liquid-phase reaction sintering at 615 °C in vacuum for 20 min, improved the ultimate tensile strength, 0.2% yield strength, and hardness of the alloy by 4, 12.8, and 88%, respectively. At values of more than 9 vol% zircon, percent elongation and the dimensional changes of the sintered composites remained virtually unchanged. At a critical volume fraction of zircon, between 0.03 and 0.05, a sharp rise in hardness was observed. Microstructural and mechanical property analysis showed that the improvement in the mechanical properties is attributable largely to the load-bearing ability and intrinsic hardness of zircon, rather than to particulate dispersion effects. A good distribution of the dispersed zircon particulates in the matrix alloy was achieved.

Keywords
particulate composites, sintering, structural material

1. Introduction

METAL MATRIX composite materials (MMCs) are some of the most exciting technologies being explored today. Early research considered continuous fiber reinforcement (Ref 1), which was very soon restricted to applications requiring the ultimate in performance because of the cost of continuous fibers, complex fabrication methods, and limited fabricability. This led to the development of discontinuous fiber and particulate reinforcements. The particulate composites of light metals are in their commercial production stage now because of their low cost, high modulus and strength, high wear resistance, and easy fabricability (Ref 2, 3). The powder metallurgy (PM) technique in the synthesis of MMCs found initial use because of the difficulty in wetting ceramic particles with molten metals, and this critical factor still generates problems in solidified composites (Ref 2, 4). The advantages of solid-state processing over solidification processing in the fabrication of composites include processing at lower temperature regimes, resulting in less interaction between the matrix and the reinforcement and more possibilities to control the interface (Ref 5, 6); improved compositional and microstructural control and homogeneity; refined grain size and supersaturated solid solution (Ref 7, 8); and fiber orientation during the extrusion or rolling of a mixture of matrix powder and fibers (Ref 6). Less costly routine maintenance and tremendous improvements in mechanical properties of interest also make the PM route favorable, especially considering the cost of equipment and tool wear in solidification processing, as well as boundary precipitates and inherent porosity (Ref 9, 10).

Owing to the level of porosity attainable, higher-technology applications for the military, aerospace, and special automobiles require parts (both heavy-duty and of intricate shapes) made via the high-cost hydrostatic and isostatic compaction, hot dynamic compaction, or explosive compaction methods, while the relatively low-cost methods of single compaction, double compaction, and mechanical deformation following hot pressing are used to produce parts for electromechanics, automobiles, and low-duty machinery (Ref 11). The effective use of aluminum alloy matrix composites (AMCs) in transportation and industry has been attributed to their relatively low cost and excellent combination of properties, such as high strength-to-weight ratio, good corrosion resistance, high thermal conductivity, and good fabricability (Ref 12). On the other hand, the development of particulate composites synthesized by PM has made AMCs an economically viable material (Ref 13, 14).

Zircon, $ZrSiO_4$, is known to be chemically very stable. Considerable energy is required to break the bonds necessary for its reduction into zirconia and zirconium metal (Ref 15, 16). It is known to be abundantly available in Australia, India, South Africa, the USA, and the former USSR, with the current world production estimated at more than 800,000 metric tons per year. Because of its availability, its inherently high stability even at high temperatures, the energy needed, and the expensive process equipment required to reduce the orthosilicate compound, more research is presently focused on alternative economic uses (Ref 17-19). Works on zircon-containing composites are emerging (Ref 20-22). Different cast AMCs reinforced with particulates of zircon are being studied for various applications (Ref 13, 23, 24). These works have only adopted the liquid metallurgy route in their investigations. The use of liquid metal as a starting material seems, in a few cases, to provide an inexpensive means of processing MMCs. However, concerns about possible contamination of the matrix material

J.U. Ejiofor and **R.G. Reddy**, Dept. of Metallurgical and Materials Engineering, The University of Alabama, P.O. Box 870202, Tuscaloosa, AL 35487, USA; and **B.A. Okorie**, Dept. of Metallurgical and Materials Engineering, Enugu State University of Technology, P.M.B. 01660, Enugu, Nigeria.

while in liquid form, particle segregation due to the relatively high specific gravity of zircon, and the prohibitively high melting points usually make the liquid metal technique inappropriate.

This paper describes a simple, inexpensive, double-compaction PM route in the synthesis of Al-13.5Si-2.5Mg alloy composites reinforced with zircon particles for light- to medium-weight applications. The mechanical and physical properties of these composites were determined and analyzed, and the parallel microstructural features were studied.

2. Experimental Procedure

2.1 *Materials*

Conventional, double-compaction PM processing was adopted. The principal steps involved pretreatment of the particulate materials, elemental blending and mixing of the matrix powders and the reinforcements, pressing into near-net shape green compacts, delubrication (or presintering), and reaction sintering of the compacts. A detailed description of these stages has been given elsewhere (Ref 11). Figure 1 provides a flowsheet of the procedures. The matrix alloy powders, aluminum and silicon, were supplied by the Aluminum Powder Co. Ltd. (ALPOCO), West Midlands, England, and by Goodfellow, Cambridge, England, respectively. They were analyzed for elemental compositions using atomic absorption spectroscopy, and the results are as shown in Table 1. The aluminum powder was produced by air atomization; the silicon, by comminution and milling.

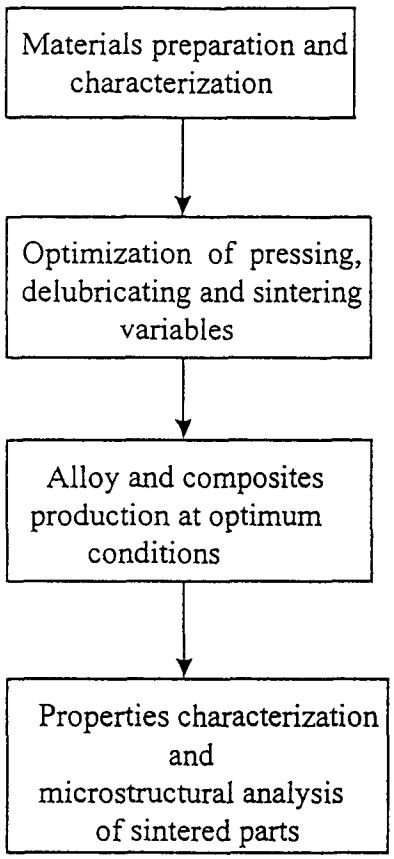

Fig. 1 Processing method flowsheet

The zircon sand used in this work was a by-product in the mineral processing of an alluvial deposit of cassiterite ore from Amalgamated Tin Mines, Nigeria. Sacrillegious materials were removed from the sand by washing it in 1.5 *M* NaOH solution. The sand was comminuted for size reduction and subsequently annealed for stress relief. The shape of the washed particle which was taken using computerized image analyzer attached to a Jeol JXA-840A SEM is shown in Fig. 2(a). For composition analysis, a sample was digested in a solution of HF + HNO_3, heated and sealed in a Teflon bomb. A Perkin Elmer Plasma-40 instrument (Perkin-Elmer Physical Electronics, Eden Prairie, MN) was used which works on the principle of inductively coupled plasma emission spectroscopy. The results are shown in Table 2.

Both the matrix powders and the sand were sized in an Endecott mechanical sieve shaker. Table 3 shows the particle size

Table 1 Composition (wt %) of aluminum and silicon powders

Element	Al powder	Si powder
Al	99.721	0.711
Si	0.028	98.001
Ca	...	0.276
Fe	0.150	0.314
Zn	<0.010	...
Pb	<0.010	...
Others	<0.091	0.698

Table 2 Composition of zircon sand

Element	Composition, wt %
ZrO_2	62.12
SiO_2	33.13
TiO_2	0.58
Fe_2O_3	2.01
HFO_2	1.82
SnO_2	0.09
$CePO_4$	0.10
Others	0.15

Table 3 Particle size and size distribution of the particulates

Material	Particle diameter, μm	Relative distribution, vol %	Cumulative distribution, vol %
Al	400-300	25.01	25.01
	300-200	25.86	50.87
	200-140	15.84	66.71
	140-1	33.29	100.00
Si	300-200	4.62	4.62
	200-140	3.70	8.32
	140-60	37.02	45.34
	60-0.8	54.67	100.00
Zircon sand, $ZrSiO_4$	200-140	30.80	30.80
	140-100	15.21	46.01
	100-60	20.28	66.29
	60-2	33.71	100.00

distribution of these particulates. Prior to the mixing of aluminum and silicon powders, the elemental blends were annealed under dry liquid nitrogen (dew point, –68 °C; flow rate, 2.1 L/min) at 350 °C for aluminum and at 190 °C for silicon. An x-ray surface analysis of the zircon particles was carried out and is shown in Fig. 2(b). The powder samples were analyzed for x-ray powder diffraction. The x-ray patterns for the zircon sand are shown in Fig. 2(c). A thermogravimetric analysis of

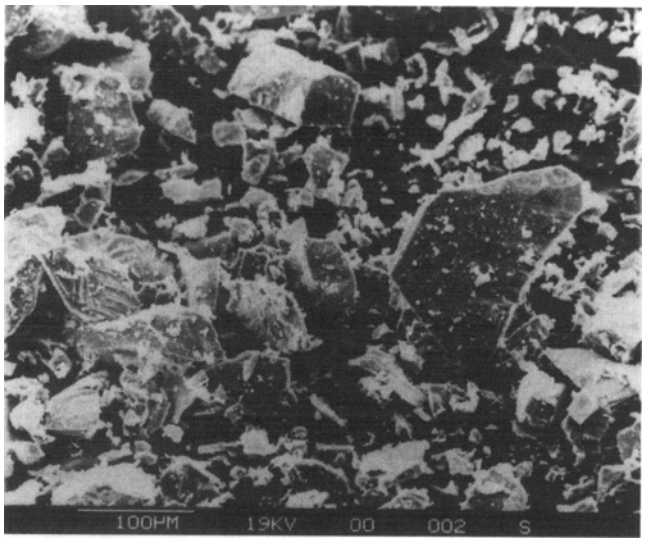

(a)

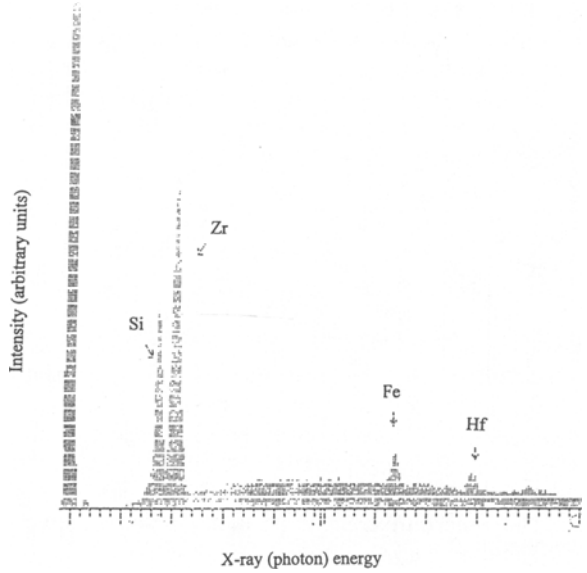

(b)

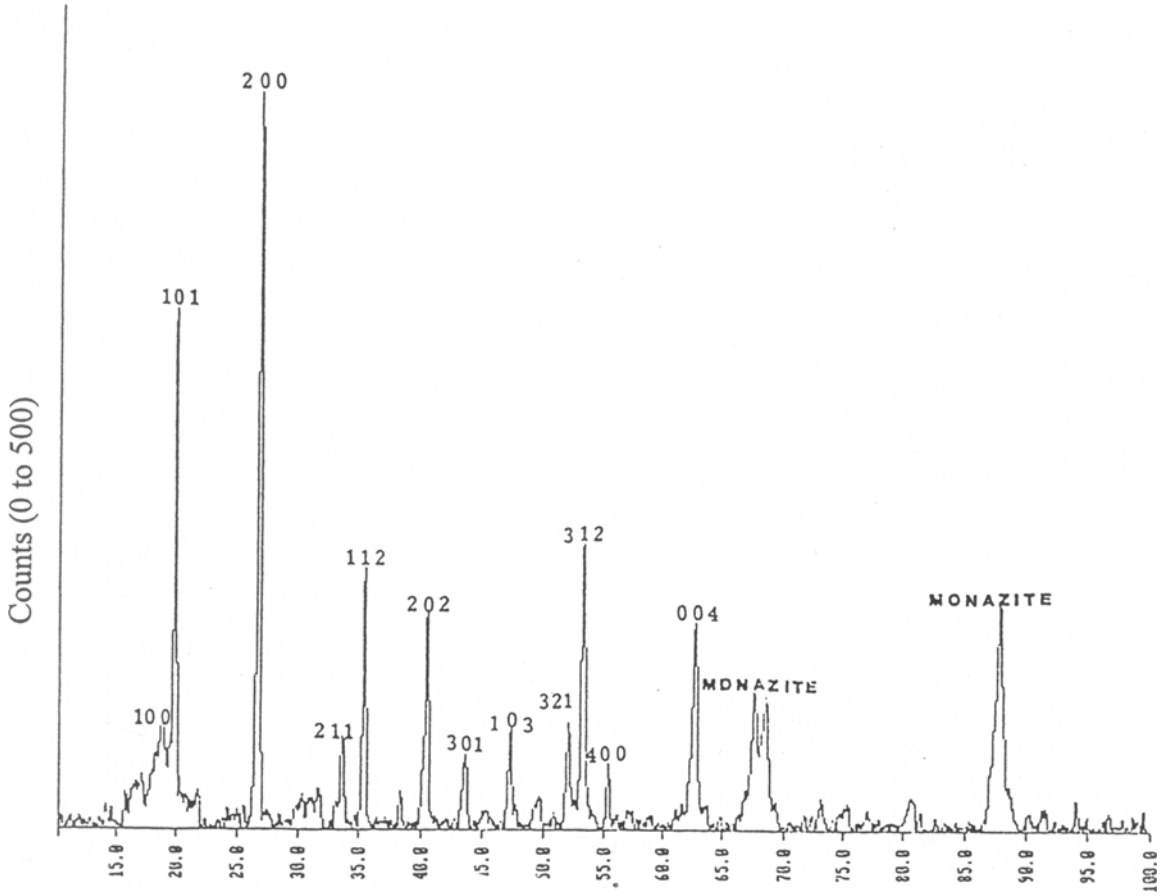

(c)

Fig. 2 (a) Zircon particles. (b) x-ray spectra of zircon particle surface. (c) x-ray pattern of zircon particles

the lubricant powders used (stearic acid and aluminum stearate) was carried out under nitrogen atmosphere to investigate the behavior of the powders during the presintering stage. At the same ramp of 10 °C/min, the matrix powders were heated to 600 °C and the lubricants to 550 °C. The thermograms are shown in Fig. 3.

The particulates were further characterized according to ASTM standards and mercury porosimetry, using the Carlo Erba Strumentazione Porosimeter 2000. These results are given in Table 4. The alloy preparation technique, composites fabrication technique, and properties testing methods, as well as the methods utilized to achieve optimal sintering conditions, are described in detail elsewhere (Ref 11).

2.2 *Alloy Preparation and Composite Fabrication*

Stearic acid (1 wt%, size 500 μm) was added to the matrix alloy elemental blend as a lubricant to aid compaction. Tensile bar specimens were produced at pressure levels 200 MPa, 250 MPa, 300 MPa, 350 MPa, 400 MPa, and 450 MPa according to Metal Powder Industrial Federation (MPIF) 10-63 requirements. A double-action hardened steel mold and punch assembly was used. The green densities of the compacts were determined and dimensions were measured prior to presintering (to remove lubricants) in a low-dewpoint (–68 °C) liquid nitrogen atmosphere at 300 °C for 1 h using a combined controlled-atmosphere/vacuum-sintering furnace. Nitrogen flow rate was maintained at 2.1 L/min and ramp at 10 °C/min. The samples were later furnace cooled to room temperature. The compacts were sintered under vacuum according to the optimal schedule: diffusion pump (tube) pressure: between 4.42×10^{-1} and 1.7×10^{-1} Pa; backing pressure: 0.08 MPa; ramp: 10 °C/min; hold temperature: 615 °C; dwell time: 20 min; cooling rate: 18 °C/min to 180 °C, then air cooled. The alloy compositions are given in Table 5.

Based on the results of the dimensional change, sintered density, ultimate tensile strength (UTS), 0.2% yield strength (YS), percent elongation, and hardness values tested (Ref 11), composite samples were compacted at 350 MPa. The Al-13.5Si alloy was reinforced with zircon at five volume fractions: 3 vol%, 6 vol%, 9 vol%, 12 vol%, and 15 vol%. Magnesium (2.5 wt%, size 100 μm) was added to the alloy as co-sinter. Tensile test-bars were compacted, delubricated in nitrogen, and sintered under vacuum in the above conditions.

2.3 *Properties Characterization*

For both the unreinforced alloys and the sintered composite parts, the heights of the sintered bars were remeasured along their gage lengths and linear dimensional change was determined. Sintered density measurements were performed by immersion technique. The UTS, 0.2% YS, percent elongation, and Vickers hardness of the sintered parts were also determined. The optical microstructure and the zircon sand dispersion in the composites were studied.

3. Results and Discussion

The matrix powders are of commercial purity (Table 1), with silicon powder being finer than aluminum (Table 3). The x-ray diffraction pattern in Fig. 2(b) reveals the presence of zircon and monazite [$(Ce, La, Th)PO_4$] peaks. This closely resembles the standard x-ray diffraction pattern of tetragonal zircon (Ref 25). As shown in Fig. 2(b), an x-ray surface analysis on zircon revealed the presence of hafnium, iron, zirconium, and silicon. From this as well as Table 2, it could be seen that iron, usually present as ilmenite ($FeTiO_3$), and hafnium occur on the surface of zircon, while monazite and rutile (TiO_3) are embedded within the grains. Lyakhovich et al. (Ref 22) have reported that a greater amount of hafnium exists on the periphery of zircon crystals than at the center. SiO_2, however, could be found both within and on the surface of the grains. On the other hand, an aluminum powder thermogram showed a negligible in-

Table 4 Characteristics of the particulates

Characteristic	Al	Si	Al-13.5Si	Zircon
Apparent density, g/cm^3	1.08	1.05	1.09	2.44
Tap density, g/cm^3	1.31	1.40	1.37	2.78
Particle density, g/cm^3	2.62	1.85	...	4.33
Total porosity, %	36.05	66.15	48.68	61.22
Specific surface area, m^2/g	1.77	0.35	4.21	0.49
Bulk density, g/cm^3	2.13	1.57	2.57	5.95
Average pore radius, nm	3853	5942	37584	25509

Table 5 Comparison of measured properties of Al-13.5Si-2.5Mg and Al-13.5Si-3.5Mg alloys each reinforced with 15 vol% zircon

Property	Al-13.5Si-2.5Mg + 15 vol% zircon	Al-13.5Si-3.5Mg + 15 vol% zircon
UTS, MPa	86	85.1
0.2% YS, MPa	50.5	46.7
Hardness, HVI	106.6	95.4
Elongation, %	1.8	1.2
Sintered density, % theoretical	88	90

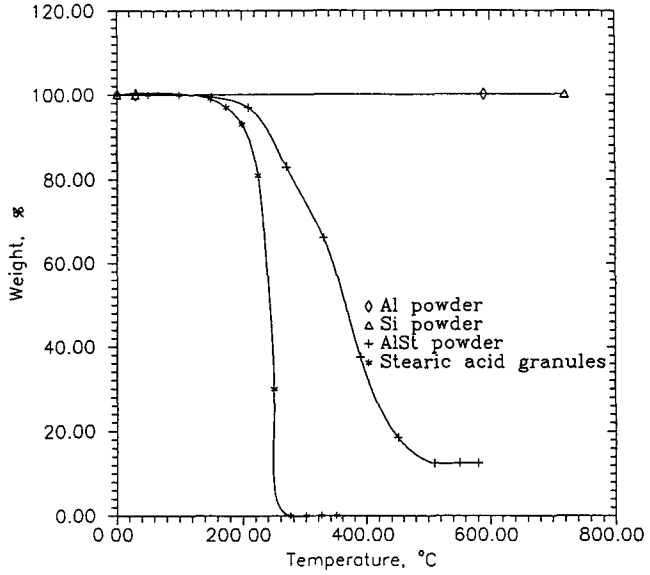

Fig. 3 Thermogravimetric analysis of matrix powders and lubricants

crease in weight due to nitriding (by 0.12%). Also, the pickup of nitrogen by silicon at about 590 °C (by 0.14%) was observed, but the effect of SiN on the mechanical properties of sintered Al-Si alloys is known to be very negligible at such an amount. The thermograms showing the behaviors of the aluminum stearate, $(C_{17}H_{35}COO)_3Al$, and stearic acid, $CH_3(CH_2)_{16}COOH$, implied that the former completely burnt off at temperatures above 510 °C and the latter at temperatures above 280 °C. This means that all lubricants are not driven off during presintering but during the subsequent sintering.

As shown in Table 4, the apparent densities of all the powders are less than their respective tap densities. This agrees with the conclusion by Hausner (Ref 26) in his work on metal and ceramic oxide powders. The high particle density of aluminum powders indicates a very low population of open and closed pores. A high surface area of the alloy elemental blend in comparison to those of aluminum and silicon powders, shown in Table 4, was observed. Increased surface areas have been reported for powder premix with spherical/angular particles of large and small sizes (Ref 27). The aluminum powders used in this work have spherical, globular structures, which are typical of air-atomized powders, and the silicon powders are angular, which is typical of milled ductile particles (Ref 11).

3.1 *Al-13.5Si Alloy*

The effects of compaction pressure on the green and sintered densities, dimensional change, and mechanical properties of Al-13.5Si alloy sintered in vacuum have been reported in an earlier work (Ref 11). The green density of the Al-13.5Si compacts increased at a decreasing rate with pressure, attributable to initial rearrangement of particles, followed by the plastic deformation of powders and the abrasion resistance of surface films present. At pressure levels above 350 MPa, green density of about 91% theoretical density was achieved. In his work on aluminum powders, Kehl (Ref 28) achieved 90% at pressures above 250 MPa. Dudas et al. (Ref 29) have reported that a density of 90 to 94% theoretical density ensures satisfactory strength in aluminum powder parts. The differences in matrix powder (aluminum is face-centered cubic and silicon has diamond structure), as well as the lubrication powders and method of lubrication, are suspected to account for the apparent variations. On the other hand, sintered density of the alloy increased marginally with compaction pressure, from 71% of theoretical value at 200 MPa to 77% of theoretical value at 350 MPa.

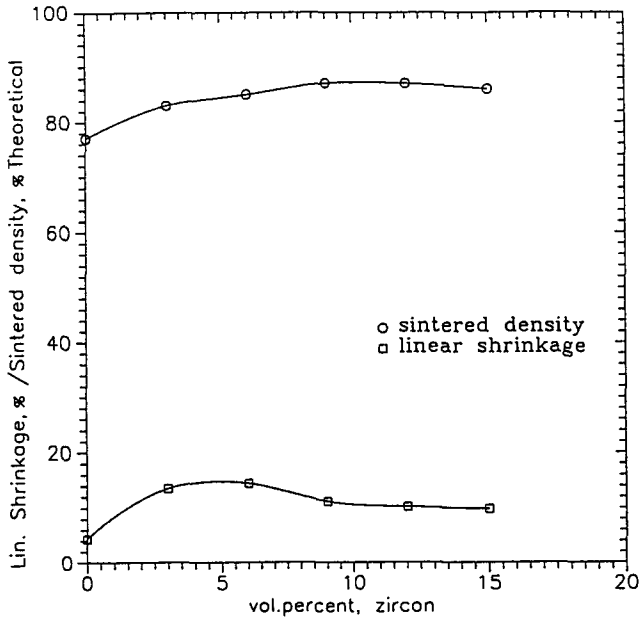

Fig. 4 Effect of zircon on linear shrinkage and sintered density of Al-13.5Si-2.5Mg alloy

Increases in compaction pressure resulted in marginal increases in the indentation hardness, UTS, and 0.2% YS of the reinforced Al-13.5Si alloys, and this has a similar behavior as their sintered density (Ref 11). This suggests that sintered density has a direct relationship with mechanical properties.

3.2 *Physical Characteristics*

Figure 4 shows that shrinkage of the sintered composite parts decreased slightly with further additions of zircon after peaking at 6 vol%. A sharp increase in shrinkage on addition of 3 vol% zircon can be observed. Apart from the low coefficient of thermal expansion of zircon, the relatively high shrinkage achieved suggested that extensive phase transformation did not occur, as no debonding was evident from the fractographic examination. Also, the sintered density of the alloy increased only marginally as additions of zircon at above 3 vol% were made. Similar effects on shrinkage and density suggest a direct relationship between the two properties.

A direct relationship between the linear shrinkage and sintered density of reaction-sintered carbon-char-reinforced aluminum composites has been reported (Ref 11). The factors suspected of influencing densification during reaction sintering include solid-state material transport through diffusion processes, evaporation and condensation of gases, wetting of various phases, particle shape, and particle size distribution. The surface modification effects of magnesium on the particulates, the relatively high surface area of the alloy, and the liquid phase sintering adopted may have been largely responsible for the density achieved. A marginal increase in the sintered density of the composite containing 0.15 V_f zircon (from 88 to 99%) following further addition of 1 wt% Mg to our matrix alloy, Al-13.5Si-2.5Mg, confirmed this effect of magnesium (Table 5). The presence of the liquid phase may have aided atomic diffusion through both lattice and grain boundary, closing porosities and improving densification. Additions of magnesium to molten aluminum alloy have been reported to assist in the dispersion and a good recovery of zircon (Ref 13). It is also possible that the presence of impurities such as niobium, titanium, calcium, and silicon promoted reactions at the particle-matrix interface, thereby enhancing densification. In this system where magnesium and aluminum are suspected to be completely dispersed, liquid may flow between particles. This will dissolve particle-particle bridges that form during the heatup period. Capillary forces acting on the particles bring about a more efficient packing. At this point, the magnitude of the interfacial energies (which determine the wetting of the solids by the liquid), the solubility of solid in the liquid, the amount of liquid present, and the particle shape and size become the influ-

encing variables for particle rearrangement (with the first two variables playing a dominant role).

3.3 *Mechanical Properties*

As shown in Fig. 5 and 6, the UTS, 0.2% YS, and hardness of the alloy increased with additions of zircon, while percent elongation was virtually unaffected. Other investigators have reported similar behaviors (Ref 13, 24). Banerji et al. (Ref 24) attributed this to the intrinsic strength and hardness of zircon, Satyanarayana et al. (Ref 24) to dispersion effects. Both workers fabricated their composites through liquid metallurgy technique. In their work, however, Pandey and Pillai (Ref 23) fabricated cast LM-O alloy (wt%: Al, 0.13Si, 0.09Cu, 0.33Fe, 0.02Ti + V, 0.01Mn + Zr + Cr) reinforced with zircon and subsequently forged the composites. They reported a progressive decrease in their mechanical properties with the additions of zircon, which was attributed to the presence of a large number of matrix cracks, particle cracks, and cracks within the vicinity of the particles. At 15 vol% zircon, the UTS and YS of the present alloy rose by 4 and 13%, respectively. The hardness of the alloy rose by a large margin of 88%. The presence of magnesium has promoted reactions at the interfaces, which also enhances dispersion of the sand in the matrix. Although the solid phase technique adopted in our fabrication may not have greatly influenced dispersion of the reinforcements because of the amount of magnesium in the composites, an additional 1 wt% Mg was introduced into the matrix alloy, Al-13.5Si-2.5Mg, resulting in an insignificantly reduced effect on the measured mechanical properties (Table 5). As a result, the factors suspected to be responsible for the improved properties are the high tensile strength and hardness (7.5 mohrs scale) of zircon and the ability of fine-size zircon particles to achieve high densification under medium to high temperatures.

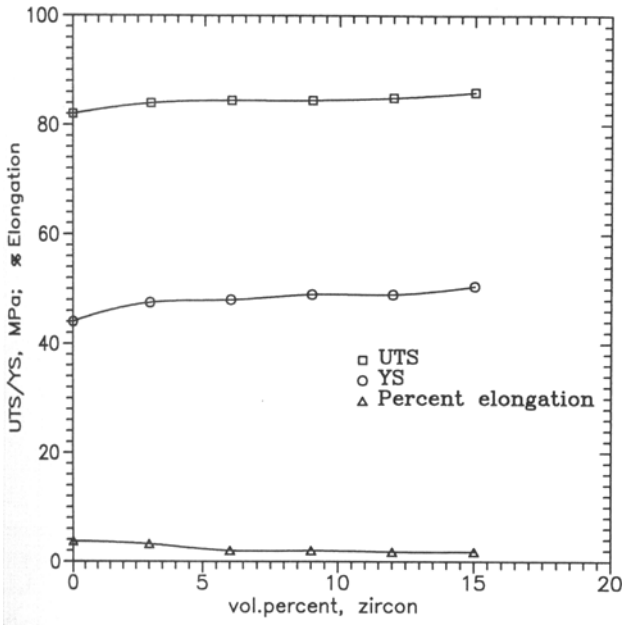

Fig. 5 Effect of zircon on tensile properties of Al-13.5Si-2.5Mg alloy

3.4 *Microstructural Features and Particle Distribution*

Figure 7 shows the optical photomicrograph of the liquid-phase-sintered, hypereutectic unreinforced alloy, Al-13.5Si, compacted at 350 MPa. Observed are the coarse lamellae (or the eutectic, α + Si) structure with α light and silicon dark, the primary silicon crystals (dark), the aluminum α-phase (light), and different aluminum compounds (or intermetallic phases) which are known to cause good wear properties, high abrasion resistance, and good heat resistance. Figures 8(a) to (c) present the optical micrographs of polished composites containing 3, 9, or 15 vol% zircon, etched in 1.5% HF solution. The dark regions around the zircon particles indicate the effect of the strong etchant used, which removed some materials at the interface. A considerable refinement of the eutectic structure can be seen, and the proeutectic aluminum also gets finer with additions of the filler phase. Natural zircons are known to contain

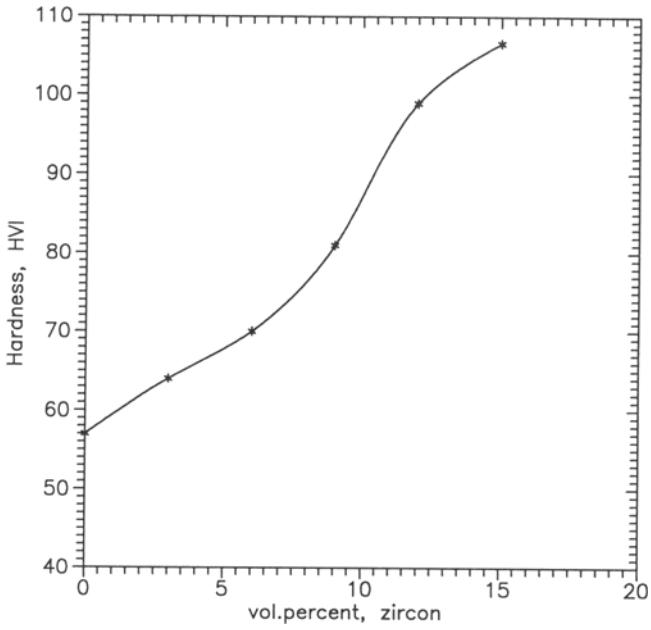

Fig. 6 Effect of zircon on hardness of Al-13.5Si-2.5Mg alloy

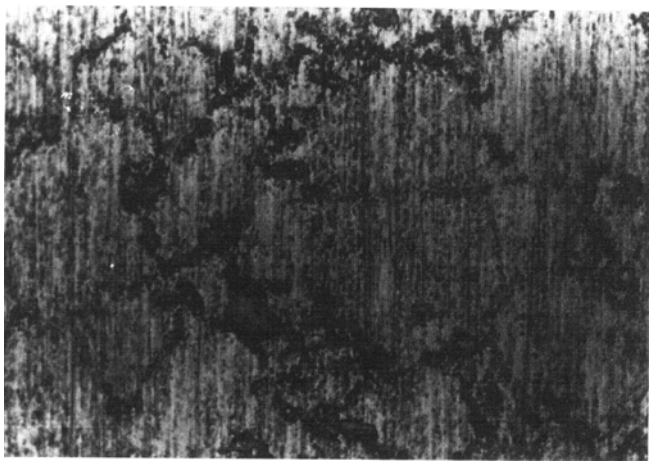

Fig. 7 Optical micrograph of vacuum-sintered Al-13.5Si-2.5Mg alloy compacted at 350 MPa.

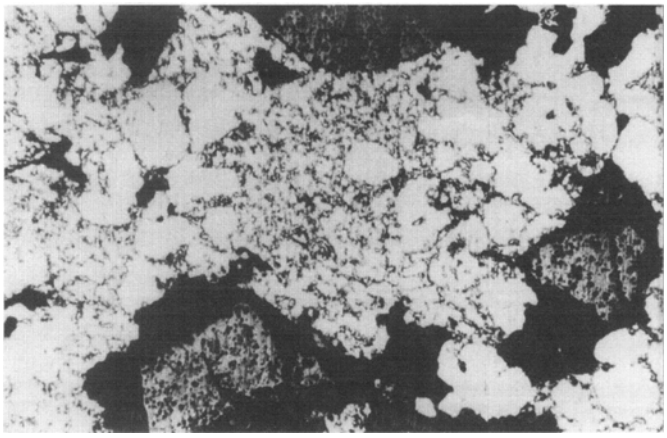

(a)

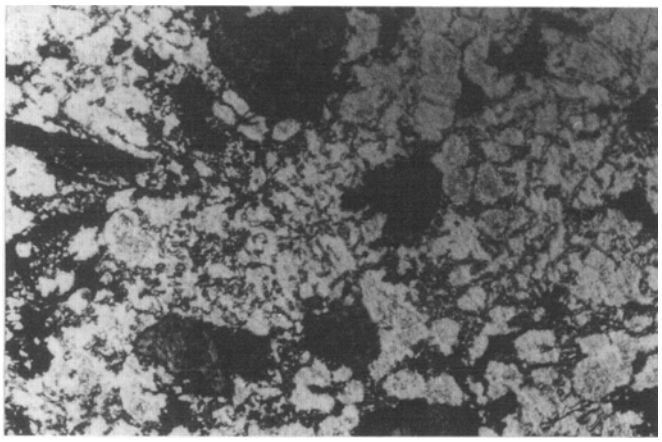

(b)

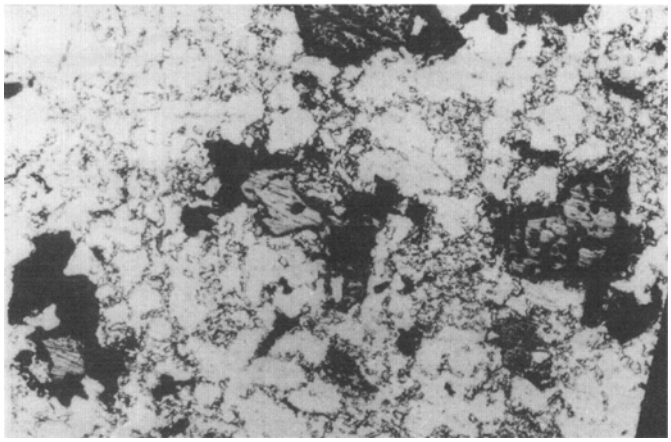

(c)

Fig. 8 Optical micrographs of Al-13.5Si-2.5Mg alloy containing: (a) 3 vol% zircon, (b) 9 vol% zircon, or (c) 15 vol% zircon. Etch: 1.5% HF

impurities (Table 2) in amounts that can lower its temperature of decomposition, influence the mechanisms of its chemical reactions, and play an important part in its sintering by producing liquid phases at the boundaries of the reaction grains. It can be seen that a fairly uniform distribution of the particles was achieved, even at a low volume fraction of the fillermaterial.

Interparticulate distance gives a fair measure of the dispersion of the particles in particulate composites. At the different sections of the bars observed under the microscope, particle segregation was not evident. From Fig. 9, it can be seen that the respective maximum frequency distribution occurs close to the mean interparticle spacing, indicating a fairly uniform distribution of the particles. Although the least interparticle distance in the composites was greater than 250 μm, the mean interparticle distance increased from 794 to 1353 μm as the volume fraction of zircon decreased from 15 to 3%.

4. Conclusions

Reduction and refinement of zircon, $ZrSiO_4$, to zirconium requires an energy-intensive and very expensive process. This work has attempted to develop a low-cost, conventional double-compaction synthesis process which exploits the high hardness of this mineral in frabricating Al-13.5Si-2.5Mg alloy composites for lightweight contact applications. A liquid-phase consolidation technique (sintering) in vacuum at 615 °C for 20 min, following presintering at 300 °C in low-dewpoint nitrogen, was found to be optimal for the alloy composite. The contact conditions of time and temperature favored the kinetics of sintering reactions in vacuum, rather than in nitrogen, to yield higher UTS, 0.2% YS, hardness, and sintered density with comparatively little dimensional change. Chemical and x-ray analyses showed that zircon minerals recovered from cassiterite ore contain compounds of hafnium, iron, niobium, titanium, and tantalum on the surface of the grains, while a significant amount of titanium-, cerium-, and silicon-bearing constituents lie embedded in the grains. Sharp increases in the linear shrinkage and sintered density of the alloy were observed when 3 vol% zircon was introduced, and this suggests that a direct relationship between the two properties also exists in such a particulate composite system. The UTS and 0.2% YS of the alloy did not increase appreciably with additions of zircon, increasing only by 4% (UTS) and 12.8% (0.2% YS) at 15 vol% zircon, and the hardness value increasing by 88% at 15 vol% zircon. However, a consistent increase in these properties was observed with additions of zircon. The hardness and the ability of the sand to bear load were found to contribute to this phenomenon. The indirect influence of the ability of fine-size zircon particle to achieve high densification under medium to high temperatures was also suspected.

Microstructural analysis revealed refinement of the matrix phases as additions of zircon were made, although this did not result in a corresponding increase in strength. The use of 1.5% HF etching solution was found to eat away materials at the high-energy regions at the matrix-sand interface, and therefore it must be considered too strong for such powder-processed materials. Analysis of the measured interparticulate distance showed that a good dispersion of the filler phase was achieved in the various composites. The tribological and thermal properties of the composites are being studied with elaborate interfacial analysis in order to understand the efficiency of load transfer under wear conditions.

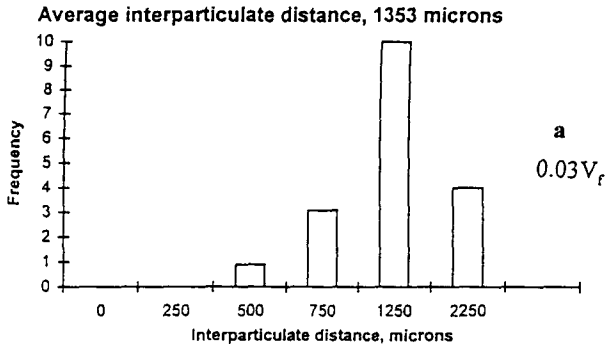

Acknowledgment

We are pleased to acknowledge the financial support of this research by the National Science Foundation, grant DMR-9696112. We also thank Prof. Brian Ralph and the staff of the Dept. of Materials Technology, Brunel University, Uxbridge, West London, for their assistance in carrying out part of this research work.

References

1. T.W. Chou, A. Kelly, and A. Okura, Fiber-Reinforced Metal Matrix Composites, *Composites*, Vol 16 (No. 3), 1985, p 187-206
2. D.J. Lloyd, Particle Reinforced Aluminum and Magnesium Composites, *Int. Mater. Rev.*, Vol 39 (No. 1), 1994, p 1-23
3. Alcan Aluminum Corp., U.S. Patent 4,786,467, 1988
4. I.A. Ibrahim, F.A. Mohamed, and E.J. Lavernia, Particulate Reinforced Metal Matrix Composites—A Review, *J. Mater. Sci.*, Vol 26, 1991, p 1137-1156
5. H.J. Rack, T.R. Baruch, and J.L. Cook, Progress in the Science and Engineering of Composites, *Proc. ICCM 4*, R. Hayashi, K. Kawata, and S. Umekawa, Ed., Japanese Society for Composite Materials, Tokyo, Japan, 1982, p 1465-1472
6. S.T. Mileiko, Fabrication of MMC, *Handbook of Composites*, Vol 4, 2nd ed., A. Kelly and S.T. Mileiko, Ed., 1986, p 221-294
7. J.S. Crompton and R.W. Hertzberg, Analysis of Second Phase Particles in a Powder Metallurgy HIP Nickel-Base Superalloy, *Mater. Sci.*, Vol 21 (No. 10), 1986, p 3445-3454
8. E.Y. Gutmanas and A. Lawley, Processing of Specialty Alloys, Composites and Intermetallics from Fine Elemental Powders, *Adv. Powder Metall.*, Vol 2, 1990, p 1-14
9. G.T. Lewis, D.M. Parkin, and F.A. Thompson, *Proc. Conf. on Forging and Properties of Aerospace Materials*, Metals Society, London, 1978, p 399
10. C.J. Lutgard, M. Chu, and M.K.F. Lin, Pore Size Distribution, Grain Growth and the Sintering Stress, *J. Mater. Sci.*, Vol 24 (No. 12), 1989, p 4403-4408
11. J.U. Ejiofor, B.A. Okorie, and R.G. Reddy, Synthesis and Property Analysis of Char Reinforced Al-Si Alloy Composites (unpublished data)
12. R. Warren, Composites, Research and Development of High Temperature Materials for Industry, *Proc. Conf. Commission of the European Communities*, Elsevier, 1989, p 153-167
13. A.M. Banerji, M.K. Surappa, and P.K. Rohatgi, Cast Al Alloys Containing Dispersion of Zircon Particles, *Metall. Trans.*, Vol 14B, 1983, p 273-283
14. S.G. Kumar, R.G. Reddy, and J. Holthus, Evaluation of Microstructure and Phase Relations in a Powder Processed Ti-44Al-12Nb Alloy, *J. Mater. Eng. Perf.*, Vol 4 (No. 1), 1995, p 63-69
15. P.V. Ananthapadmanabhan, K.P. Sreekumar, K. Veeramani, and N. Venkatramani, Influence of Some Process Variables on Plasma Dissociation of Zircon, *Mater. Chem. Phys.*, Vol 38 (No. 1), 1994, p 15-20

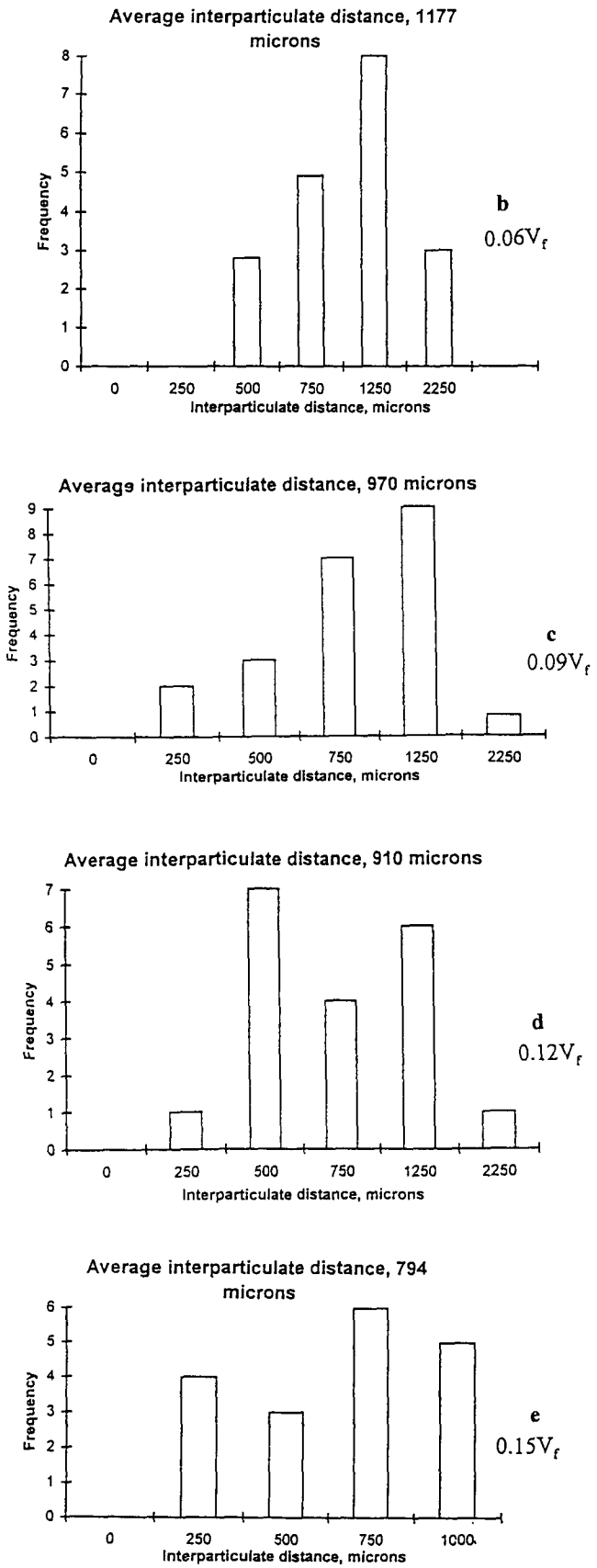

Fig. 9 Zircon particle distribution in Al-13.5Si-2.5Mg alloy at 3 to 15 vol% zircon

16. R.C. Ewing, W. Lutze, and W.J. Weber, Zircon: A Host Phase for the Disposal of Weapons Plutonium, *J. Mater. Res.*, Vol 10 (No. 2), 1995, p 243-246
17. A.B. Corradi, C. Leonelli, T. Manfredini, and C. Siligardi, Effect of Forming Pressure on the Reactivity and Microstructure of Zircon Powder Compacts, *J. Mater. Sci. Lett.*, Vol 12, 1993, p 1434-1436
18. S. DeSouza and B.S. Terry, Production of Stabilized and Nonstabilized ZrO_2 by Carbothermic Reduction of $ZrSiO_4$, *J. Mater. Sci.*, Vol 29, 1994, p 3329-3336
19. M.R. Houchin, D.H. Jenkins, and H.N. Sinha, Production of High-Purity Zirconia from Zircon, *Ceram. Bull.*, Vol 69 (No. 10), 1990, p 1706-1710
20. R.N. Singh and S.K. Reddy, Influence of Residual Stresses, Interface Roughness, and Fiber Coatings on Interfacial Properties in Ceramic Composites, *J. Am. Ceram. Soc.*, Vol 79 (No. 1), 1996, p 137-147
21. B.F. Dmitruik, O.G. Zarubitskii, and N.N. Yashchenko, Interaction of Zircon with Molten Alkali, *Ukr. Khim. Zh.*, Vol 60 (No. 5-6), 1994, p 349-353 (in English and Russian)
22. V.V. Lyakhovich, P. Uger, and P. Siman, Hafnium in Zircon from Rapakivi Granite, *Trans. USSR Acad. Sci.: Earth Sci. Sect.*, Vol 326 (No. 7), 1994, p 123-126
23. U.T.S. Pillai and R.K. Pandey, Fracture Characteristics of Al-Zircon Particulate Composites, *Compos. Sci. Technol.*, Vol 40 (No. 4), 1991, p 333-354
24. K.G. Satyanarayana, B.C. Pai, M.R. Krishnader, and C.G. Nair, Aluminum Alloy Metal Matrix Composites for Engineering Applications, *Proc. 32nd International SAMPE Symposium*, 6-9 April 1987, p 880-889
25. S.V. Ramani, S.K. Mohaptra, K.V. Gokhale, and E.C. Subarro, *Trans. Indian Ceram. Soc.*, Vol 30, 1971, p 9-56
26. H.A. Hausner, in *Handbook of Metal Powders*, A.R. Poster, Ed., Reinhold Publishing Corp., New York, 1966
27. J.E. Williams, Production of Aluminum Powders, *Powder Metallurgy, Metals Handbook*, 9th ed., Vol 7, American Society for Metals, 1984, p 125-130
28. W. Kehl, M. Bugajska, and H.F. Fischmeister, Internal or Die-wall Lubrication for Compaction of Al Powders, *Powder Metall.*, Vol 26 (No. 4), 1983, p 221-227
29. J.H. Dudas and C.B. Thompson, Improved Sintering Procedures for Al P/M Parts, *Modern Developments in Powder Metallurgy*, Vol 5, Plenum Press, 1971, p 19-36